On the source location of low-frequency heliospheric radio emissions

W. S. Kurth and D. A. Gurnett

Department of Physics and Astronomy, University of Iowa, Iowa City, Iowa, USA

Received 24 January 2003; revised 28 February 2003; accepted 20 March 2003; published 22 August 2003.

[1] We used a combination of three different types of source localization to determine the two-dimensional source positions for low-frequency heliospheric radio emissions in ecliptic coordinates. These techniques include time of flight, rotating dipole direction finding, and a comparison of received power from two widely spaced receivers. Most of the source locations are within a few tens of degrees of the heliospheric nose, although some sources are located as far as 90° from the nose. The distribution is roughly linear and aligned generally parallel to the galactic plane. We conclude that the magnetic field in the local interstellar medium is the only obvious means by which to impose an asymmetry to the set of source locations about the nose; it is likely these measurements confirm that the previously proposed model for the galactic magnetic field with a primarily longitudinal orientation parallel to the galactic plane is present just upstream of the heliosphere. The apparent sizes of the radio sources range from very small (a few degrees at the most) to a few tens of degrees. In a couple of cases the source half-angle could approach 80 degrees. We suggest that the true source size is quite small and that the larger sizes found here are likely due to scattering in the intervening medium. The fact that the apparent source size varies considerably implies that scattering in the outer heliosphere is a function of time, position, or both. *INDEX TERMS:* 2124 Interplanetary Physics: Heliopause and solar wind termination; 6954 Radio Science: Radio astronomy; 6969 Radio Science: Remote sensing; 7534 Solar Physics, Astrophysics, and Astronomy: Radio emissions; *KEYWORDS:* radio emissions, heliosphere, heliopause, radio source, Voyager

Citation: Kurth, W. S., and D. A. Gurnett, On the source location of low-frequency heliospheric radio emissions, *J. Geophys. Res.*, *108*(A10), 8027, doi:10.1029/2003JA009860, 2003.

1. Introduction

[2] In the early 1980s the two Voyager plasma wave instruments [*Scarf and Gurnett*, 1977] began detecting radio emissions in the frequency range of 1.8 to 3.6 kHz [*Kurth et al.*, 1984; *Gurnett et al.*, 1993; *Gurnett and Kurth*, 1995] which have been suggested by these authors to have a source in the vicinity of the heliopause resulting from shocks associated with global merged interaction regions interacting with the interstellar medium. Observations of these radio emissions from the two Voyager receivers are summarized in Figure 1. In this figure we display the power relative to background as a function of frequency (ordinate) and time (abscissa) using the color scheme defined by the color bar on the right. See *Gurnett and Kurth* [1996] and *Kurth and Gurnett* [1997] for reviews of these emissions. Note that particularly above the narrow line at 2.4 kHz (a power supply interference tone) there are subtle but definite differences in the received power for some of the components of the radio emission as observed by the two spacecraft. During the time interval of these observations the two Voyager spacecraft were moving outward from the Sun in the general direction of the nose of the heliosphere (the direction from which the apparent interstellar wind is coming) as shown in Figure 2. At the beginning of 1995 the angle between the Voyager 1 velocity vector and the direction to the nose was about 10°; for Voyager 2 this angle was ~83°. In this paper we attempt to combine information on the location of the source of these radio emissions derived from three different techniques to constrain the source location to relatively small regions.

1.1. Time-of-Flight Technique

[3] The first good determination of the heliocentric distance to the source region came from time-of-flight considerations by *Gurnett et al.* [1993] and *Gurnett and Kurth* [1995]. These authors pointed out that the two major radio emission events which had occurred as of that time (beginning in 1983 and 1992) came some 412 and 419 days, respectively, after the two strongest Forbush decreases on record at neutron monitors on Earth. The assertion was that the shock and associated turbulence comprising global merged interaction regions causing the Forbush decreases traveled for more than 400 days before reaching a relatively high-density region in the vicinity of the heliopause where the shocks then caused the generation of the radio emissions. Based on reported shock speeds for these two events and modeling by *Steinolfson and Gurnett* [1995] of the shock speed in the subsonic solar wind beyond the termination shock, *Gurnett and Kurth* [1995] arrived at source distances ranging from 110 to 160 AU from the Sun. The range of distances comes from varying estimates for the

0148-0227/03/2003JA009860$09.00

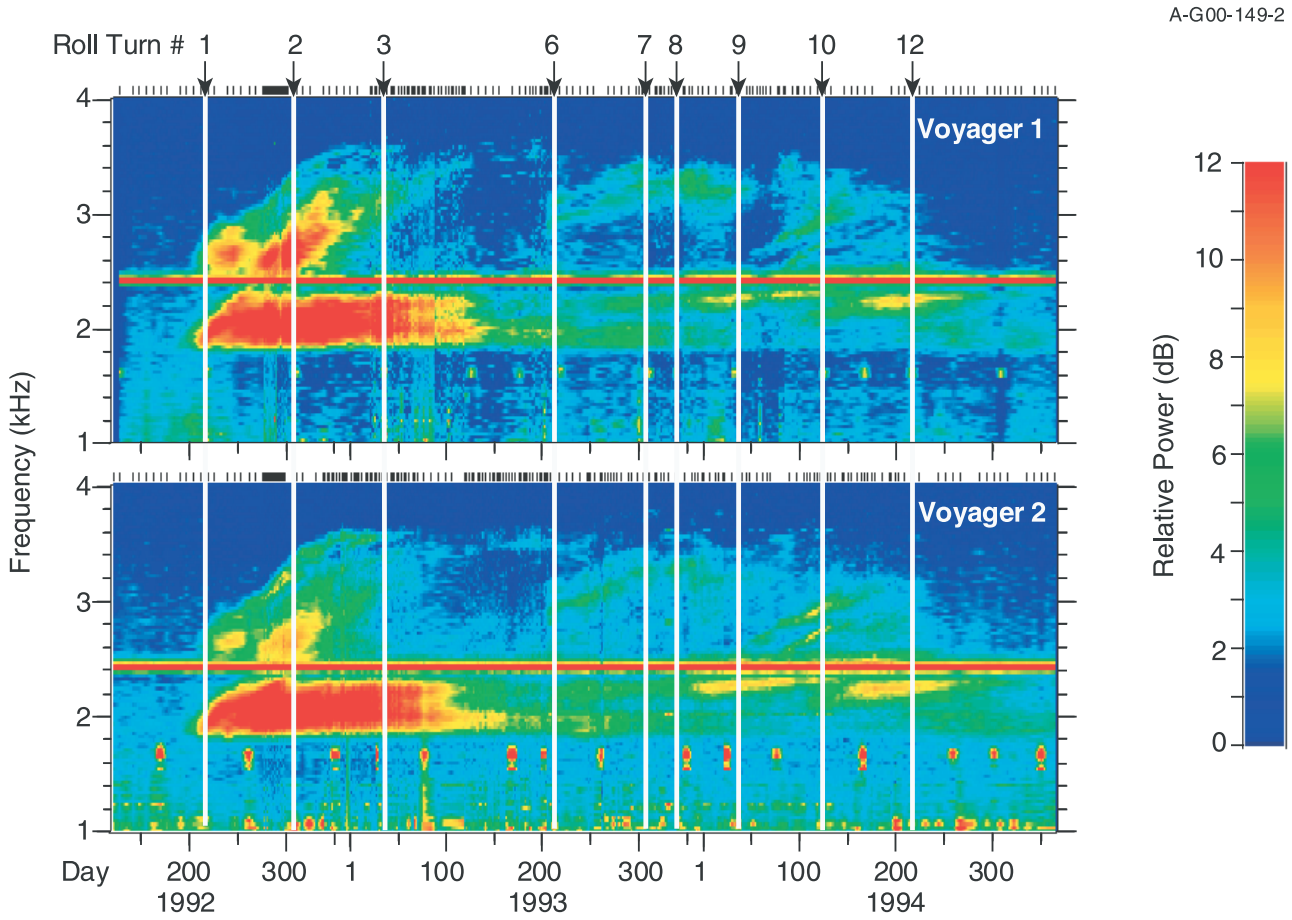

Figure 1. Frequency-time spectrograms from Voyagers 1 and 2 showing subtle differences in the intensity of low-frequency heliospheric radio emissions as viewed from the different vantage points of these two spacecraft. The vertical white lines indicate times when Voyager 1 roll turn maneuvers were used by *Gurnett et al.* [1998] to find the directions to the radio source using the rotating dipole direction-finding technique.

observed shock speeds and uncertainties in the modeled shock speeds beyond the termination shock.

1.2. Rotating Dipole Direction-Finding Technique

[4] *Gurnett et al.* [1993, 1998] utilized the rotation of the Voyager 1 plasma wave antenna during calibration rolls of the spacecraft to further determine the source of the radio emissions detected in the 1992 to 1994 time frame. This technique, sometimes called the rotating dipole technique, uses the modulation of the signal strength as a function of antenna orientation to determine the plane containing the source. Figure 3 shows a drawing of the Voyager spacecraft with its principal axes identified as well as the plasma wave science antennas. As a dipole antenna rotates, the received signal varies due to the nonuniform response of the antenna. When the signal is at a minimum, the source lies in the plane determined by the rotation axis of the spacecraft and the dipole axis. *Gurnett et al.* [1998] define Ψ as the azimuthal direction of the source measured about the spacecraft roll axis (the Z_{SC} axis in Figure 3) relative to the direction to the nose of the heliosphere ($\Psi = 0$) as determined by *Ajello et al.* [1987] at an ecliptic latitude of $\beta = 5°$ and longitude of $\lambda = 254°$. A second parameter which comes from the analysis of the roll-modulated signal is the depth of the null in the signal, or modulation index *m*. *Gurnett et al.* [1998] defines the modulation index as the ratio of the peak-to-peak intensity of the roll modulation to the maximum intensity. The modulation index is determined by three factors: (1) the angle of the source from the spin axis of the spacecraft, (2) the source

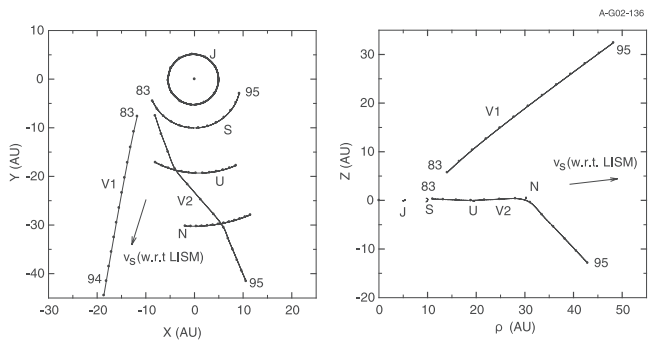

Figure 2. Trajectories of the two Voyager spacecraft (V1, V2) in 1950 ecliptic coordinates through the period 1983–1995. Note that during the time interval of 1992–1995, the spacecraft were separated by ~40 to 60 AU. Also shown are the trajectories of Jupiter (J), Saturn (S), Uranus (U), and Neptune (N). An arrow shows the direction of the velocity of the Sun $\mathbf{v}_s$ with respect to the local interstellar medium (LISM).

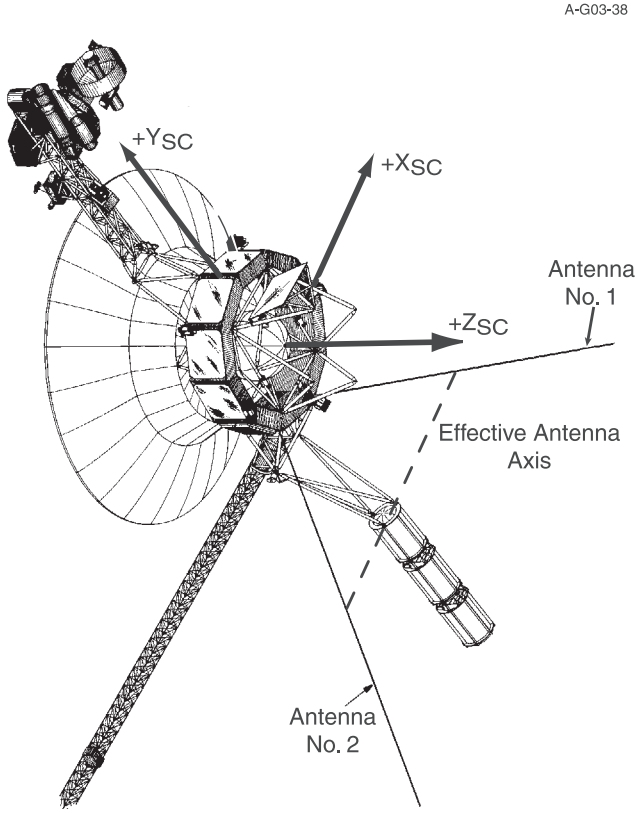

Figure 3. A drawing of the Voyager spacecraft showing the principle axes of the spacecraft (labeled X_{SC}, Y_{SC}, and Z_{SC}), the two plasma wave science antenna elements, and the effective dipole orientation for long wavelengths. The response of the plasma wave antenna system is greatest for sources perpendicular to this effective antenna axis and zero for point sources collinear with it.

size, and (3) scattering of the waves between the source and the spacecraft. If the angle between the source and the spin axis is 0°, then there will be no spin modulation for a circularly or randomly polarized source. The modulation will be greatest for a source at 90° to the spacecraft rotation axis. The modulation index will be maximum for a point source and will go to zero for an extended source (one which subtends 2π steradians). The modulation index will also be decreased by scattering [*Cairns*, 1995, 1996; *Armstrong et al.*, 2000] which tends to broaden the apparent angular size of the source. The first of these factors bears on the direction to the source; hence it can be used to further restrict the possible source locations to the extent that the source is not too large and the scattering is not too great. We pursue this below. The results of the rotating dipole direction-finding technique for several roll maneuvers during the 1992–1994 time frame are given in Table 1 using the numbering scheme of *Gurnett et al.* [1998] but not including three maneuvers for which no modulation and hence no direction was found. The roll maneuvers are also identified using the same numbering scheme in Figure 1.

1.3. Relative Intensity Technique

[5] *Kurth and Gurnett* [1997] pointed out that subtle differences can be seen in the amplitude of various components of the heliospheric radio emission as observed from the two Voyager spacecraft. Inspection of the two spectrograms in Figure 1 reveal that especially for the drifting features greater than about 2.4 kHz there are some features which are more visible on Voyager 1 than on Voyager 2 and vice versa. *Kurth and Gurnett* [2001] have developed a technique which uses these relative intensity differences to further restrict the source locations. Basically, a given ratio of observed power at the two spacecraft can be used to determine a surface upon which a source would have to lie. Because a dipole antenna is not uniformly sensitive in all directions, variations in signal strength as viewed by two observers can also be due to different antenna orientations; hence the technique includes consideration of the different antenna orientations for the two Voyager spacecraft. A summary of the technique is given below.

[6] In principle, we can use the relative power detected by two widely separated observers such as the two Voyager spacecraft to determine a locus of possible locations of a radio emission source. If we assume omnidirectional sensors, then the basic equation is

$$\left(\frac{r_2}{r_1}\right)^2 = \frac{P_1}{P_2} \tag{1}$$

where r_1 and r_2 are the distances to the source from Voyager 1 and 2, respectively, and P_1 and P_2 are the observed power fluxes at the two spacecraft. The geometry is illustrated in Figure 4. In this simple case, one can calculate the relative power at the two spacecraft for any given hypothetical source position. For any given ratio of received power, one can determine a surface upon which the source must lie. In three dimensions, each of these surfaces is a sphere surrounding one of the spacecraft (the one receiving the most power) except for the limiting case

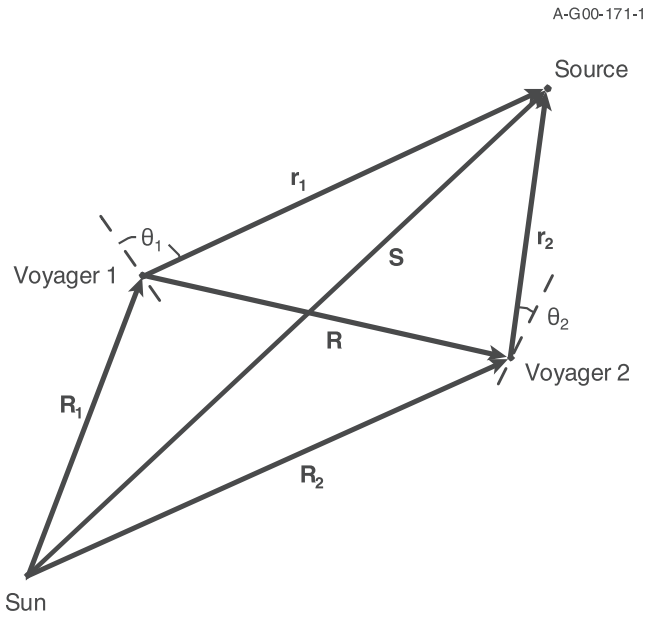

Figure 4. A diagram describing the geometry of the relative intensity measurements, including the angles between the effective Voyager dipole antenna axis and the direction to the source.

of no difference (0 dB) which gives a plane perpendicular and bisecting the line segment between the two spacecraft.

[7] In reality, the two Voyager plasma wave instruments use electric dipole antennas which are not omnidirectional but which have a response (to a point source) of the form $a(\theta) = \sin^2\theta$, where θ is the angle between the antenna axis and the direction to the source **r**. When the source is collinear with the antenna axis, the response is zero for a point source; when the source is in a direction perpendicular to the antenna axis, the response is one. Hence equation (1) must be modified in the following way to account for the dipole antenna patterns of the two spacecraft.

$$\frac{a_1(\theta_1)}{a_2(\theta_2)}\left(\frac{r_2}{r_1}\right)^2 = \frac{P_1}{P_2} \tag{2}$$

[8] Because of the antenna pattern effect, the shape of a surface defined by a constant ratio of received power becomes considerably distorted and is no longer a sphere. It should be noted that even though the Voyager antenna system consists of two physical elements extended at right angles to each other, their response is the same as a linear dipole for wavelengths much longer than the antenna. This effective antenna axis is parallel to a line connecting the midpoints of the two elements. For the Voyager antennas this direction is parallel to the spacecraft x axis, i.e., perpendicular to both the high gain antenna axis and the magnetometer boom as shown in Figure 3.

[9] Because of a failure in the Voyager 2 flight data system which affected the spectrum analyzer intensity measurements in the 1.0 to 56.2-kHz frequency range, channels in the appropriate frequency range (1.78 and 3.11 kHz) for detecting the heliospheric radio emissions cannot be used for relative intensity measurements. We must use, instead, the wideband receivers on the two spacecraft for this comparison.

[10] The wideband receivers utilize automatic gain control circuitry and the gain information is not returned in the telemetry; hence there is no absolute calibration for these data. We utilize the fact that the lowest-frequency (2-kHz) component of the emission never shows roll modulation (at least for the interval studied herein) to suggest that the source must be nearly isotropic [*Gurnett et al.*, 1998]. Therefore it is likely the intensity of this component is nearly identical at the two spacecraft and can be used as a cross-calibration signal. Furthermore, the sensitivities of the two receivers are basically identical and are thought to be at maximum gain in the very quiet outer heliosphere at least when spacecraft interference sources are at a minimum. In many cases we note that this lowest-frequency component has an identical intensity when comparing spectra from the two spacecraft. Using the 2-kHz component as a calibration source, then, we can compare the intensities of the more transient higher-frequency components.

[11] Figure 5 shows a detailed spectral comparison for wideband data averaged over 20 s from day 224 of 1992. The amplitude scale is proportional to power flux but the absolute value is arbitrary. If there is a difference in the observed amplitude of the lowest-frequency component, we multiply one of the spectra by a constant to make them the same, based on the reasoning above that the low-frequency component makes a reasonable cross-calibration signal. For the case in Figure 5 the 2-kHz components are almost identical in amplitude as measured by both instruments; hence no multiplication was necessary. In this example, Voyager 1 observes a signal centered near 2.7 kHz that is approximately 3.3 dB larger than that observed by Voyager 2. In determining the received power ratio, we subtract the background noise from the observed power for each receiver and then find the ratio. The background noise is determined by drawing a line between minima in the spectrum at frequencies above and below the heliospheric radio emissions. Since the interference in this frequency range is almost always narrowbanded and the radio emissions are limited to the frequency range of 1.8 to 3.6 kHz, this technique should give a reasonable noise level. Note that for some of the later cases some multiplication of one or the other of the spectra is necessary. We believe this is due to variations in the low-frequency (<1 kHz) interference levels which are set primarily by the operation of the tape recorder used to record the wideband data and gyros which may or may not be running during a particular observation. The variable interference spectrum can change the gain of the receiver and its noise level.

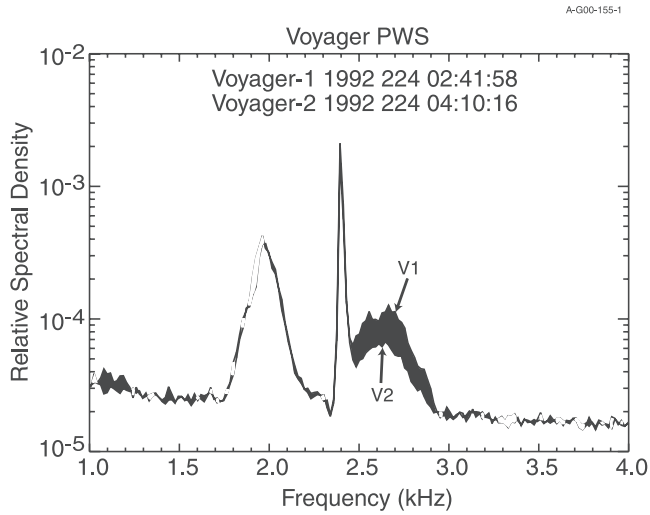

Figure 5. A comparison of the spectrum observed by the two Voyagers on day 224, 1992 at nearly identical times. For the broad band centered on 2.7 kHz, Voyager 1 observes a signal which is approximately 3.3 dB greater than observed by Voyager 2.

[12] In principle, the use of equation (2) and the observed power ratio defines a surface upon which the source must lie. Rather than perform a search in three-dimensional space for this surface, however, we have chosen to make use of the results of the rotating dipole direction-finding measurements from *Gurnett et al.* [1998] (summarized in Table 1) to limit our search to the plane of the source as determined by that method. By performing a coordinate transformation from the solar ecliptic frame into one based on the (X′-Y′) plane defined by the rotation axis of Voyager 1 and the direction to the source (from the rotating dipole technique), we can then compute the intersection of the appropriate relative power contour in the plane of the source. This is shown in Figure 6 for the rotating dipole determination of day 220 of 1992, just a few days before the spectral comparison in Figure 5 was obtained. In order to understand

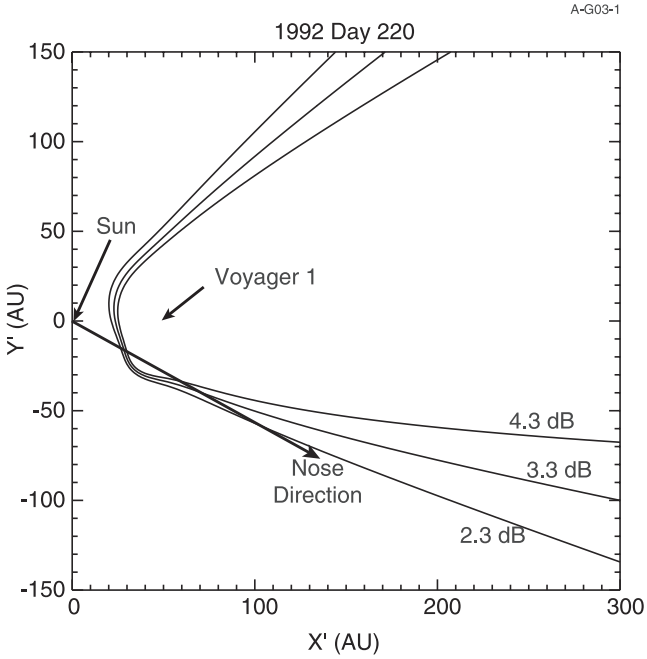

Figure 6. Contours of constant relative intensity using the spectral comparison in Figure 5. The contours are the intersection of surfaces defined by the observed relative intensity and the plane of the source determined by the rotating dipole technique on day 220, 1992 [*Gurnett et al.*, 1998]. The X′-Y′ frame is that defined by the Voyager 1 roll axis (X′) and the location of the source centroid.

the effect of errors of the order of a dB or so in determining the relative power at the two spacecraft, we have included contours for ratios of 2.3, 3.3, and 4.3 dB. This provides an opportunity to see how the results could change if the ratio were shifted up or down by 1 dB. A line labeled "nose" indicates the projection of the nose of the heliosphere into the plane of analysis, with an assumed distance of 150 AU. Notice that this direction is very close to all three contours for an extended distance. *Gurnett et al.* [1998] found the source to be consistent with the direction to the nose, so it is comforting to see the contours lie close to the nose position, as well.

[13] Because the contours in Figure 6 extend for a large distance beyond the nose, the relative amplitude source location method does not, in this case, provide a useful restriction in the distance to the source. Note also that both the rotating dipole technique and the relative amplitude method have ambiguities, e.g., there is no a priori way of eliminating possible source locations along the 3.3 dB contour in the upper half of the plane. It should further be recognized that the feature centered at 2.7 kHz in Figure 5 does not coincide exactly with the frequency channel used by *Gurnett et al.* [1998] for the rotating dipole technique. However, the spectral response of that channel does include the high-frequency wing of the 2.7-kHz line, and we assume that the entire band is generated in the same general location.

[14] The wideband measurements used for the relative intensity measurements are typically only available once per week on each spacecraft and do not correspond exactly with the times when the rotating dipole direction finding is carried out. Nevertheless, because the heliospheric radio emission spectrum evolves very slowly, on time scales of days [*Kurth and Gurnett*, 1997], we have chosen times as close as possible to the those listed in Table 1 for which to determine the relative intensity of the emissions from the two Voyager spacecraft. The results are given in Table 2. Note that *Gurnett et al.* [1998] use the 3.11-kHz channel on Voyager 1 for the rotating dipole technique. This spectrum analyzer channel has an effective bandwidth of 298 Hz, but the filters are not ideal square filters and have significant response outside of this bandwidth. Hence in Table 2 we note the center frequency of the band for which we have measured the relative amplitude.

2. Source Localization Using Combined Techniques

[15] None of the three techniques described in the preceding section are very restrictive in the determination of the source location when used alone. The time-of-flight determination only gives a distance to the source. The rotating dipole technique determines the plane of the source (although the modulation index can further restrict the source to certain regions in this plane as described below). Finally, the relative intensity technique determines a surface upon which the source must lie in order to explain the relative intensities observed by the two spacecraft. However, we have selected times for the relative intensity determination which correspond fairly closely in time with those used by *Gurnett et al.* [1998] for the rotating dipole determinations. Further, all of the source locations are subject to the

Table 1. Summary of Rotating Dipole Results[a]

		Voyager 1 Location			Roll Axis Direction				
Roll Turn	Day, Date	R(AU)	β, deg	λ, deg	β, deg	λ, deg	Ψ, deg	*m*	α, deg
1	220, 7 August 1992	49.4	33.5	245.0	−33.7	63.7	−10.4 ± 3.0	0.29	57.4
2	311, 6 November 1992	50.3	33.5	245.3	−33.0	64.8	33.4 ± 1.6	0.08	73.6
3	36, 5 February 1993	51.2	33.6	245.6	−33.4	66.8	21.8 ± 1.6	0.15	67.2
6	218, 6 August 1993	53.0	33.7	246.0	−33.9	64.8	43.1 ± 8.5	0.06	75.8
7	309, 5 November 1993	53.9	33.7	246.3	−33.2	65.8	−52.4 ± 3.5	0.13	68.9
8	336, 6 December 1993	54.2	33.7	246.4	−33.2	66.4	−63.1 ± 0.6	0.52	43.9
9	35, 4 February 1994	54.8	33.8	246.5	−33.5	67.7	−85.1 ± 3.4	0.15	67.2
10	125, 5 May 1994	55.7	33.8	246.7	−34.3	67.2	31.9 ± 1.3	0.28	58.1
12	217, 5 August 1994	56.6	33.8	247.0	−34.1	65.8	58.9 ± 10.7	0.61	38.7

[a]After *Gurnett et al.* [1998].

Table 2. Spectral Ratios

Associated Roll Turn	Day, Date	Voyager 1 Position			Voyager 2 Position			Frequency, KHz	Power Ratio, dB
		R, AU	β, deg	λ, deg	R, AU	β, deg	λ, deg		
1	224, 11 August 1992	49.4	33.5	245.0	37.9	−10.5	283.0	2.7	3.3
2	308, 3 November 1992	50.3	33.5	245.3	38.6	−11.2	283.1	3.2	−2.1
2′	308, 3 November 1992	50.3	33.5	245.3	38.6	−11.2	283.1	2.6	3.6
3	40, 9 February 1993	51.2	33.6	245.6	39.3	−11.9	283.3	3.15	7.0
6	215, 3 August 1993	53.0	33.7	246.0	40.7	−13.3	283.6	3.1	1.6
6′	215, 3 August 1993	53.0	33.7	246.0	40.7	−13.3	283.6	2.95	−0.8
7	306, 2 November 1993	53.9	33.7	246.3	41.4	−13.9	283.7	3.2	−0.3
8	337, 3 December 1993	54.2	33.7	246.4	41.6	−14.2	283.8	3.25	2.5
9	42, 11 February 1994	54.8	33.8	246.5	42.1	−14.6	283.8	3.2	3.7
10	123, 3 May 1994	55.7	33.8	246.7	42.8	−15.2	284.0	3.25	4.5
10′	123, 3 May 1994	55.7	33.8	246.7	42.8	−15.2	284.0	2.95	−1.0
12	221, 9 August 1994	56.6	33.8	247.0	43.6	−15.8	284.2	3.1	−0.3

time-of-flight determination of the heliocentric distance albeit with some complicating factors for times much later than the beginning of the event in 1992. Hence we attempt in this section to combine the results of all of these techniques for the several time periods reported by *Gurnett et al.* [1998].

[16] We begin by presenting the results of the relative intensity determination only in the plane determined by the rotating dipole technique as was done by *Kurth and Gurnett* [2001]. Since the latter technique determines the plane of the source, we show the contour of observed relative intensity in the same plane. In addition, we make the assumption that the source is a point source and scattering effects can be ignored so that the modulation index can be used to restrict regions of the source plane because the observed modulation index is too large to be consistent with sources that are close to the spacecraft rotation axis. As noted by *Kurth and Gurnett* [2001] and explained below, the reduction in modulation index by either an extended source or scattering or both tends to bring the source closer to the plane perpendicular to the rotation axis (that is, closer to the spin plane) in order to explain the observed modulation index. Finally, we add arcs in the designated plane centered at the Sun which have radii of 110 and 160 AU since this is the range of distances to the source based on the time-of-flight analysis by *Gurnett and Kurth* [1995]. The distances to the source for those determinations in 1992 are subject primarily to uncertainties in the shock speed as described by *Gurnett and Kurth* [1995]. However, for determinations in 1993 and 1994 one has to consider that the triggering shock continues to propagate to considerably larger distances from the time onset of the radio event to the time of the distance determination being used. There are two basic ways to proceed: (1) assume the shock continues to move at constant speed during the time from the beginning of the radio emission event in 1992 to the time in question, hence extending the distance to the source, or (2) assume that later components in the emission seen in Figure 1 are other shocks embedded in the global merged interaction region and are following the primary shock, hence, probably begin interacting with the source region at about the same distance. *Kurth and Gurnett* [1997] discuss different ways of interpreting the complex spectrum seen in Figure 1 which are of relevance to this consideration. For simplicity, we will adopt assumption 2 as the inner edge of the source region, but realize that the outer limit of the source could potentially be significantly further for the later events.

[17] Figure 7 presents the combined results of all three of the source location determinations described above for the time period near roll turn 1. To begin, Figure 7 contains the same contours as those shown in Figure 6 in the source plane determined by the rotating dipole technique. The cross-hatched regions in Figure 7 represent locations in the source plane where the source would seem to be ruled out by the modulation index reported by *Gurnett et al.* [1998]. In Figure 7 the spin plane includes Voyager 1, is parallel to the Y′ axis, and is perpendicular to the plane of the illustration. If the source was directly in the spacecraft spin plane, was a point source, and there was no scattering, the modulation index would be 1. If we assume for the moment that the last two of these assertions are true, then the modulation index is entirely determined by the angle of the source from the spin plane as described by the following equation.

$$\alpha = \cos^{-1}\sqrt{m} \tag{3}$$

[18] The cross-hatched region is limited by lines at $\pm\alpha$ from the spin plane. Hence the source would lie on one edge of the cross-hatched regions extended from the Voyager 1 position. We indicate the value of α for each of the roll turns in the last column of Table 1. Any extension of the source size or scattering (both of which reduce the modulation index) would have the effect of moving the source closer to the spin plane and away from the cross-hatched region for a given modulation index. *Cairns* [1995, 1996] estimated the scattering would be so great that basically no roll modulation should have been seen by Voyager at all. However, *Armstrong et al.* [2000] have reestimated the magnitude of scattering and find it consistent with the modulation observed. We do not know the source size. Some of the spectral features in Figure 1 have bandwidths of order 100 Hz, which implies that the waves are being generated in a region where the plasma frequency (hence plasma density) variation is quite limited. We discuss the apparent source size below.

[19] Finally, in Figure 7 we have drawn arcs centered on the Sun with radii of 110 and 160 AU based on the minimum and maximum distances to the source based on the time-of-flight determination [*Gurnett and Kurth*, 1995]. The source must lie between these arcs.

[20] Figure 7, then, contains all the information we currently have to identify the source location of the 2.7-kHz component of the heliospheric radio emission near day

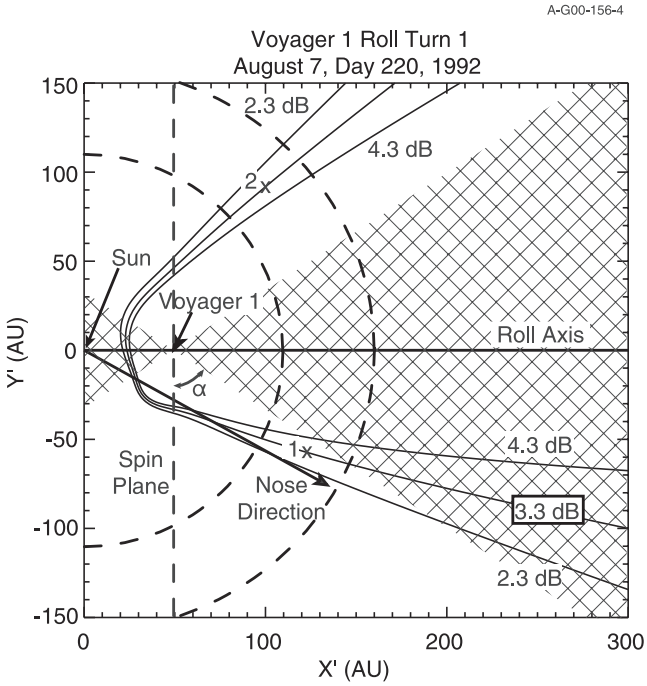

Figure 7. A summary of source location information available near the day 220, 1992 roll turn maneuver 1. The plane shown is the plane of the source as defined by the rotating dipole technique. The two dashed arcs at 110 and 160 AU represent the range of distances to the source from the time-of-flight determination from *Gurnett and Kurth* [1995]. The contours are the same as the ones in Figure 6, with the 3.3 dB contour representing the locus of source locations which would lead to the observed 3.3 dB relative intensity. The hatched regions are source locations which are forbidden by the magnitude of the modulation index reported by *Gurnett et al.* [1998]. The vertical dashed line is the intersection of the spacecraft spin plane with the plane of the source; the angle α between this plane and the cross-hatched region is determined from the modulation index determined in the rotating dipole technique (see text). The two "x" symbols are positions which are consistent with all of the above source location techniques. Position 1 is designated as a "prime" source location because it is closest to the heliospheric nose, where one would expect the first contact between an outward-moving GMIR and the region at or beyond the heliopause. Position 2 is also consistent with all of the source location information but is less likely to be the true source; both the rotating dipole technique and relative intensity techniques have ambiguities which result in a second possible source location. We have identified position 2 as the ambiguous solution.

220 of 1992. There are two regions in this figure that are consistent with all available information. The first, labeled 1, lies in the lower half of the plane between the dashed arcs, on the 3.3-dB contour. This location is consistent with the spin modulation measurement by being outside of the cross-hatched area. Remarkably, this region is also consistent with the location of the heliospheric nose projected into this plane. The other source, labeled 2, is in the upper portion of this plane, also near 135 AU, near the 3.3-dB contour, and outside the cross-hatched region. We can now take these positions, identified by the x's in the figure, and transform them into ecliptic coordinates. Location 1, which lies near (122 AU, −58 AU) in the X′-Y′ frame transforms into a position in ecliptic coordinates (R, β, λ) of (135 AU, 8°, 249°). Location 2 at (100 AU, 91 AU) transforms into (135 AU, 74°, 221°).

[21] Figure 8 shows comparative spectra from wideband measurements obtained on day 308 of 1992 from the two Voyager instruments. In this example, there are two emission bands above 2.4 kHz, one that is quite broad and centered near 2.6 kHz and a weaker and narrower one near 3.2 kHz. As can be seen in the comparative spectrum, Voyager 1 observes the 2.6-kHz emission more strongly than does Voyager 2 by about 3.6 dB, whereas Voyager 2 observes the 3.2-kHz band to be stronger by about 2.1 dB. Both bands overlap the response of the Voyager 1 3.11-kHz channel. In Figure 9 we compile the various types of evidence for source location as we did in Figure 7. In this case, however, we have plotted contours for −1.1, −2.1, and −3.1 dB with the −2.1 dB contour representing the received power ratio at 3.2-kHz (the negative sign indicates the Voyager 1 to Voyager 2 received power ratio is less than 1), and also a contour at +3.6 dB representing the received power ratio at 2.6 kHz. So in this case, there are four potential source locations identified. Source location 1 represents a source consistent with the −2.1 dB (3.2-kHz source) contour and close to the nose direction. Source location 2 is the ambiguous counterpart to source 1 on the −2.1 dB contour near the top of the illustration, where there is virtually no difference between the three negative contours. Source location 3 is on the 3.6-dB contour consistent with the 2.6-kHz band and close to the nose direction. The ambiguous alternate to source location 3 is identified as source location 4, not far from source location 2 but on the 3.6-dB contour. Notice that all four locations are "allowed" in the sense that they do not fall within the cross-hatched

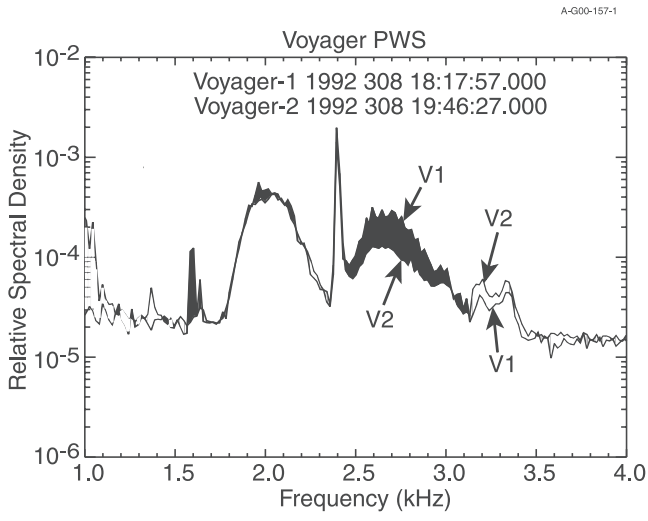

Figure 8. A comparison spectrum from day 308, 1992 illustrating two frequency components near 3.11 kHz. For the lower frequency component, centered near 2.6 kHz, Voyager 1 observes a signal which is approximately 3.6 dB stronger than observed by Voyager 2. The feature centered on 3.2 kHz is approximately 2.1 dB stronger as observed by Voyager 2.

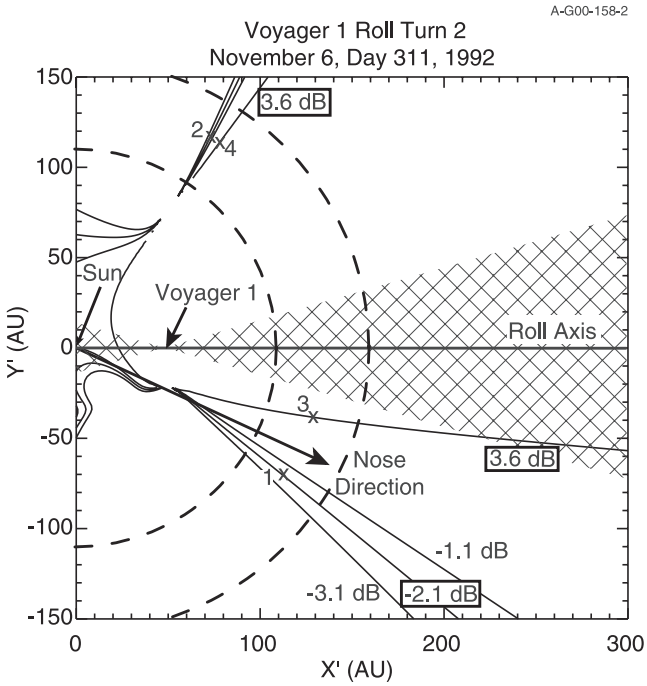

Figure 9. A summary of source location information near the day 311, 1992 roll turn 2 similar in format to Figure 7. In this case, four source locations are identified. Positions 1 and 2 are on the −2.1 dB contour representing the 3.2-kHz feature which is observed more strongly by Voyager 2. Positions 3 and 4 are associated with the 2.6-kHz feature which is observed more strongly by Voyager 1. Positions 1 and 3 are considered "prime" since they are closest to the heliospheric nose; positions 2 and 4 are the ambiguous alternates for these.

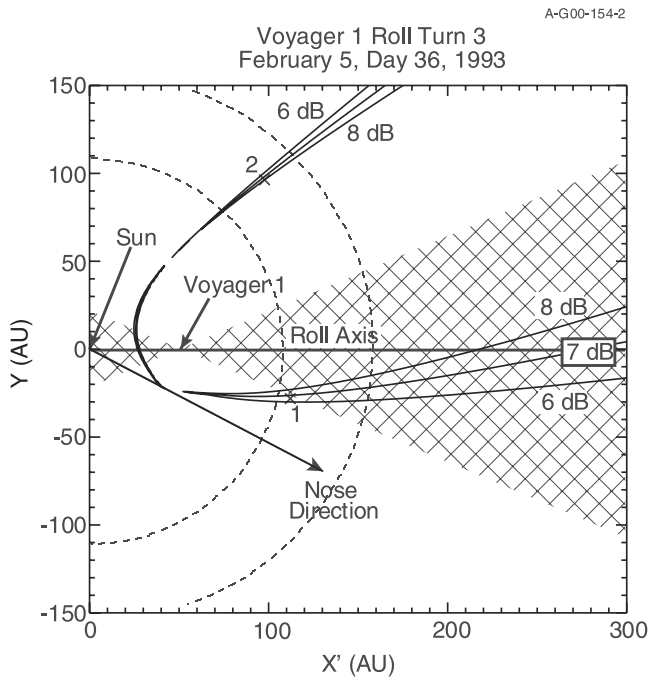

Figure 10. A summary of source location information near the day 36, 1993 roll turn 3. In this case the prime source at position 1 is right on the border of the cross-hatched region; hence the apparent source size is very small. In fact, the distance to the source would seem to be limited by the fact that the 7-dB contour intersects the cross-hatched region closer to the 110-AU arc than the 160-AU arc.

region set by the modulation index for roll turn 2 [*Gurnett et al.*, 1998]. We have again chosen locations approximately half-way between 110 and 160 AU along each of the contours. As before, the positions of these four source locations can be transformed into ecliptic coordinates. These are (133 AU, 11°, 271°) for source 1, (137 AU, 47°, 168°) for source 2, (134 AU, 22°, 260°) for source 3, and (137 AU, 47°, 171°) for source 4.

[22] We constructed plots in the same format as Figures 7 and 9 for the other roll turns for which *Gurnett et al.* [1998] were able to determine a plane containing the radio emission source. These are given in Figures 10–16. We record in Table 3 the positions determined from similar considerations as for the cases in Figures 7 and 9. In general, two source locations are allowed by the results, and both solutions are provided in the table. For those cases (like those illustrated in Figures 8 and 9) which exhibit two bands near 3.11 kHz, four source locations are derived, two for each band. Also included in the table are the center frequencies of the spectral components used in the determination for comparison with Figure 1. There are not likely two real source regions for any given determination; one is the "true" source, while the other is an ambiguous alternate. As will be discussed further below, we have called the source location of an ambiguous pair closest to the heliospheric nose direction the "primary" source and the other location the "ambiguous" solution. In almost all cases, the

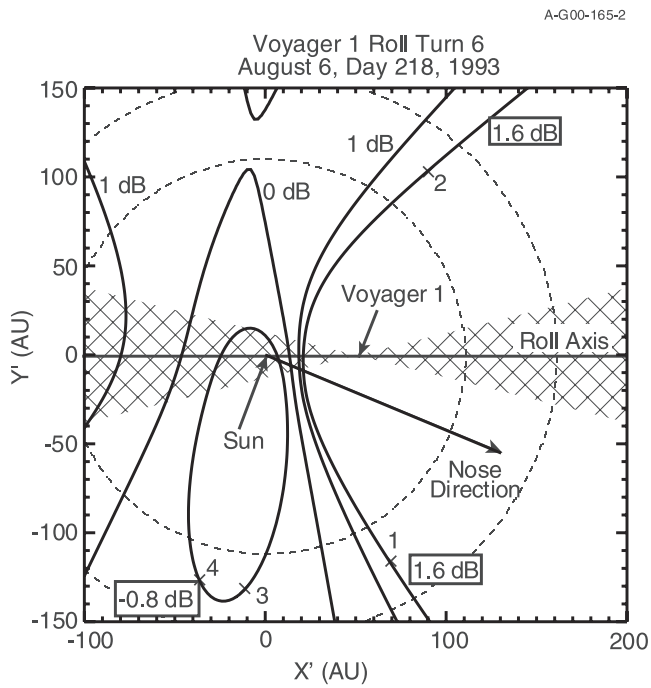

Figure 11. A summary of source location information near the day 218, 1993 roll turn 6. This is another case with two frequency bands (3.1 kHz corresponding to positions 1 and 2, and 2.95 kHz corresponding to positions 3 and 4). The great distance of these sources from the cross-hatched region suggests a large apparent source size due to significant scattering.

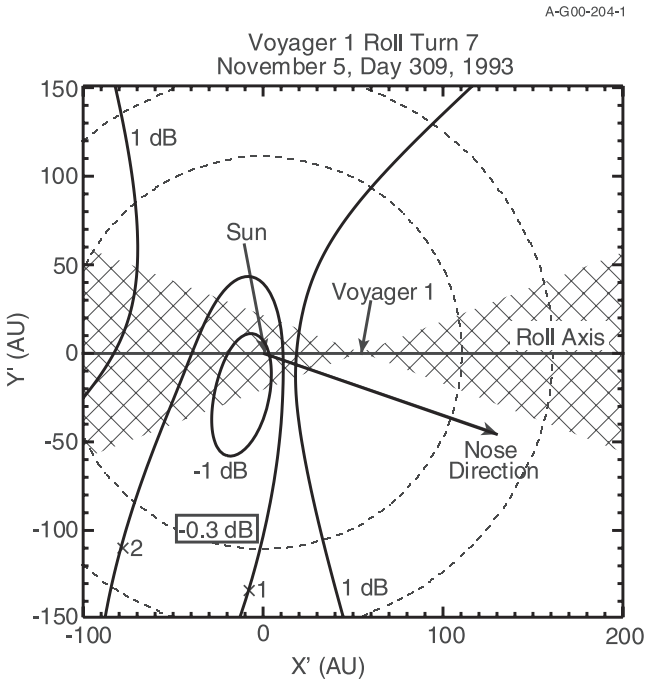

Figure 12. A summary of source location information near the day 309, 1993 roll turn 7. This is another case where the source is very far from the cross-hatched region, suggesting significant scattering.

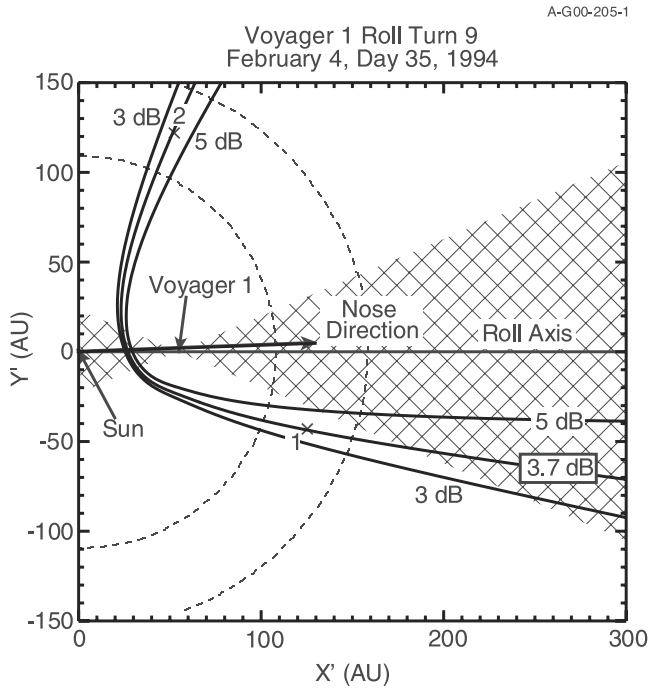

Figure 14. A summary of source location information near the day 35, 1994 roll turn 9.

"primary" source is also close to an edge of the cross-hatched region.

[23] While Figures 10–16 are similar to Figures 7 and 9, some comments on individual situations should be made. In Figures 10, 15, and 16 (roll turns 3, 10, and 12), the contours representing the position of the source closest to Voyager 1 intersect the cross-hatched region between the arcs at 110 and 160 AU. Since, in principle, the source

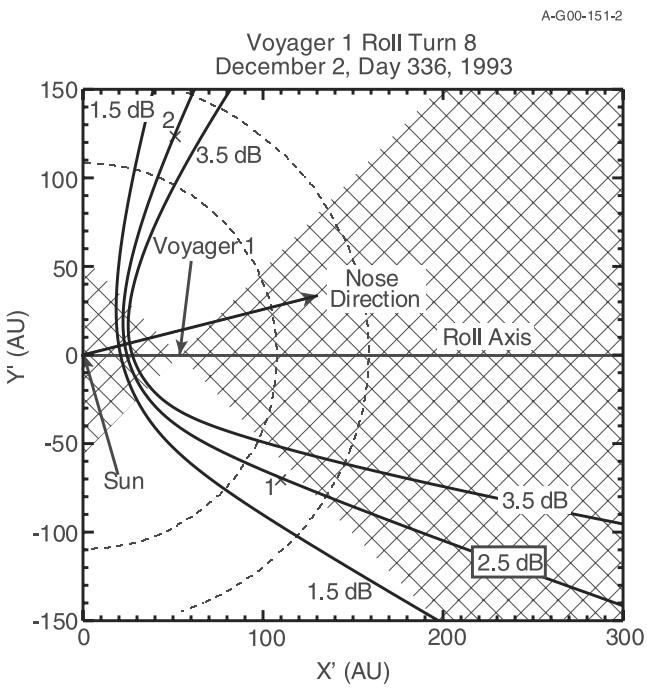

Figure 13. A summary of source location information near the day 336, 1993 roll turn 8. Since positions 1 and 2 are approximately equidistant from the nose direction, position 1 was selected as "prime" because of its proximity to the cross-hatched region.

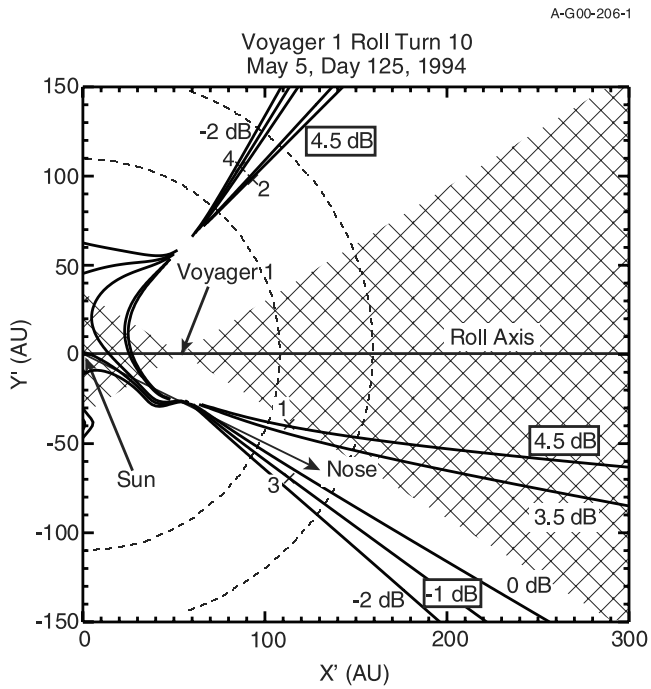

Figure 15. A summary of source location information near the day 125, 1994 roll turn 10. Notice that position 1 (corresponding to the 3.25-kHz component) is located right at the edge of the cross-hatched region. Position 3 corresponds to the 2.95-kHz component.

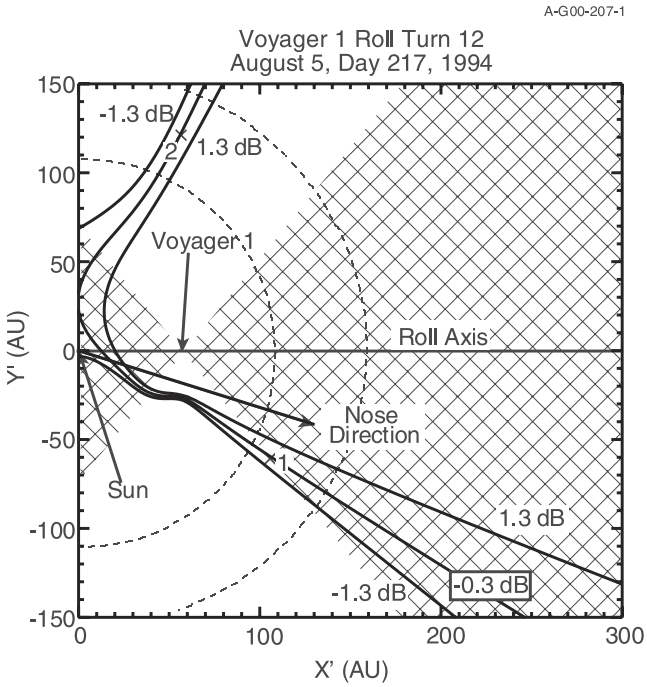

Figure 16. A summary of source location information near the day 217, 1994 roll turn 12. Again, this source is located very close to the edge of the cross-hatched region suggesting a very small apparent source size and little scattering. The distance to this source appears to be limited by the intersection of the contour with the cross-hatched region.

cannot be within the cross-hatched region and be consistent with the observed modulation index, we have located the source at the edge of the cross-hatched region. This, in fact, provides an upper limit on the source distance in these three cases. Roll turns 6 and 7 (in Figures 11 and 12, respectively) represent the opposite situation. Here, the source contours are well separated from any edge of the cross-hatched region. This means the source lies relatively close to the spacecraft spin plane and that the modulation index is quite small. We conclude that the apparent source size is quite large for these cases. We will return to this point below.

[24] We caution the reader that there are numerous and substantial sources of error in the source locations presented in Table 3. The rotating dipole phase angles from *Gurnett et al.* [1998] have errors ranging from 0.6° to 10.7°, which at ~90 AU from the spacecraft spin axis correspond to positional errors ranging from 1 to 17 AU perpendicular to the line of sight. The error in the relative intensity determination is largely unknown since our assumption of the low-frequency component as a viable cross-calibration source may not be correct. However, given this assumption, we believe we can determine the intensity ratio to within about 0.5 dB and, by inspection of Figure 7, this corresponds to an uncertainty in the direction to the source as viewed from Voyager of the order of a few degrees. The results from the other cases are similar; hence one may conclude that the uncertainty in the in-plane source direction is of the same order as those determined by *Gurnett et al.* [1998] for the rotating dipole determination of the source plane. The errors in the distance to the source are the same as those given by *Gurnett and Kurth* [1995] or between 110 and 160 AU before consideration of propagation distance from the onset of the event. The modulation index is also subject to errors, primarily because in the determination of *m*, *Gurnett et al.* [1998] had to subtract a noise level from the observed signal, and there is some uncertainty in this value. However, we do not use *m* to determine a direction directly, only for a consistency check, so its error is less relevant.

[25] Another source of error, not mentioned above, has to do with the assumption of a point source in the model for the antenna response used in the received power ratio analyses. As the source size increases, the antenna response becomes less directional until for a source of 2π steradians it is uniform. *Baumback* [1976] examined the variation in the modulation index for a uniformly illuminated source disk as a function of source size and angle of the source from the spacecraft spin plane α. Using the situation for source location 1 in Figure 7 as an example, we note that the elevation of this source from the Voyager 1 spin plane is about 51°, whereas the modulation index would place a point source on the edge of the cross-hatched region which is at an angle of 57° from the spin plane. Using Figure 15 of *Baumback* [1976], one can see that a source with a half-angle size of about 33° will result in a modulation index of 0.29 (as measured by *Gurnett et al.* [1998]) and an elevation angle $\alpha = 51°$. Hence a source with half-angle size of about 33° can explain the difference between the observed source location and the source elevation angle assuming a point source. We suggest that such a source size (with a diameter of order 100 AU at a distance of 100 AU) is inconsistent with the narrowband emissions observed and that the implied source size is actually a combination of the true source size (much less than 33° half-angle) and scattering, although there is no way to determine what portion of the apparent size is due to scattering. At least for the case of roll turn 1 the effect of an extended apparent source does not seem to cause an error in direction more than several degrees or similar in magnitude to the other sources of error noted above. Many of the sources for at least one frequency band in each determination are within a few to several degrees of a cross-hatched edge, suggesting the apparent source sizes are of the order of a few tens of degrees and the separation between the edge and the source location is indicative of the errors associated with the point-source assumption made herein. In roll turns 3, 10, and 12

Table 3. Determined Source Locations

Associated Roll Turn	Frequency, kHz	Primary Solution			Ambiguous Solution		
		R, AU	β, deg	λ, deg	R, AU	β, deg	λ, deg
1	2.7	135	8	249	135	74	221
2	3.2	133	11	271	137	47	168
2′	2.6	134	22	260	137	47	171
3	3.15	113	22	255	136	59	188
6	3.1	139	−21	223	138	68	189
6′	2.95	133	−53	201	137	−63	181
7	3.2	123	−45	191	138	−61	143
8	3.25	135	50	284	135	−19	200
9	3.2	134	38	270	139	−2	186
10	3.25	121	19	260	135	53	184
10′	2.95	137	10	268	135	53	177
12	3.1	120	22	275	140	26	169

the primary source locations are right on the edge of the cross-hatched regions; hence the apparent source size must be very small for these, since their elevation angle from the spin plane accounts for their modulation index, alone. The use of the point-source approximation in these cases is unquestionable. However, for roll turns 6 and 7 the primary source locations are both far from the cross-hatched edge and relatively close to the Voyager 1 spin plane. Given the small values for m, it follows that these sources must have a rather large apparent source size. Using Figure 15 of *Baumback* [1976], we estimate a half-angle width of order 80 degrees. Such a source, if a uniformly illuminated disk, would result in a very small modulation index, even for a source near the spin plane.

[26] Since apparent source sizes of order 80 degrees strongly violate the point-source assumption, we re-calculated the relative intensity contours assuming omnidirectional antennas, which should reasonably approximate the response to a source nearly 2π steradians in extent. For roll turn 7 the -0.3 dB contour shifts very little from its position in Figure 12. On the other hand, using the omnidirectional response approximation for roll turn 6 moves the 1.6 dB contour (and solution 1) all the way over to the edge of the cross-hatched region closest to the nose direction. The -0.8 dB contour rotates in such a way that solution 3 moves closer to the cross-hatched region opposite the nose direction, even further than it already was. Having solution 1 on the edge of the cross-hatched region then violates the assumption of a large apparent source (hence the omnidirectional response function) since the modulation would be entirely explained by its angle out of the spin plane. We conclude that the positions for roll-turn 6 are questionable at this point.

3. Summary of Results and Discussion

[27] Table 3 summarizes the results of combining the various direction-finding approaches presented in Figures 7 and 9–16. In particular, we note the "primary" source location in ecliptic coordinates as well as that of its "ambiguous" mate. Where two frequencies are used in the relative intensity analysis, there are two "primary" and two "ambiguous" sources. Admittedly, there remains an unresolved ambiguity, although we believe our choice of the source closest to the nose and a cross-hatched edge as "primary" is warranted, especially for the earlier determinations, simply on the grounds that the propagation of an approximately spherically symmetric global merged interaction region (GMIR) outwards would result in contact with the nose of the heliopause first and other locations later in time. Figure 17 displays the source locations as a function of ecliptic latitude and longitude (epoch 1950), with the direction to the nose shown for reference. Because for each roll turn as many as four potential source locations are determined, we have encoded these so as to enable the reader to relate each determination to the specific roll turns. First, all sources from a given roll turn number are encoded with that number. Second, those determinations which were chosen as "primary" are shown in black; these correspond to the odd-numbered sources in Figures 7 and 9–16. The red numbers represent the "ambiguous" solutions. Third, the second frequency sources are primed. Hence a red, primed 6 would be the "ambiguous" mate for the second frequency (2.95 kHz) determination in roll turn 6.

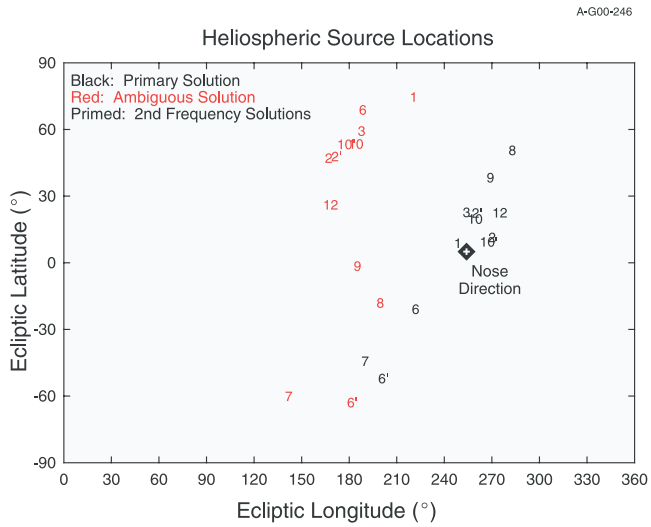

Figure 17. A summary of the source locations presented in Figures 7 and 9–16 rotated into [1950] ecliptic coordinates. The direction to the heliospheric nose is also indicated. Each source location is indicated by the roll turn number specified in Figure 1 and consistent with the numbering scheme used by *Gurnett et al.* [1998]. The "prime" solutions are indicated in black and the "alternate" solutions are in red. The second frequency solutions (as indicated in Table 3) are indicated with primes. Notice that the "prime" solutions are mostly clustered near the nose direction but are elongated in a linear fashion away from the nose direction instead of being randomly clustered around it.

[28] It is useful to examine the source locations in Figure 17 with the original data in Figure 1 in mind. As pointed out by *Gurnett et al.* [1998], the roll turns occur over time and tend to be grouped by the spectral features occurring during general intervals in time. For example, roll turns 1–3 occur during the first set of transient events in the radio emission activity shown in Figure 1. Roll turns 6–9 occur during a second general set of transient features. A last set of spectral features appears during the interval of roll turns 10 and 12. To some extent, the locations of the "prime" sources in Figure 17 represent this grouping. All of the "prime" sources associated with the first 3 roll turns are clustered very close to the nose direction. In fact, the low-frequency source from roll turn 2 ($2'$) appears to drift to a frequency consistent with the feature whose source is determined in roll turn 3, and these two sources are very close to each other in Figure 17. The directions derived from turns 10 and 12 are close to the nose, as well. That the later events have a source very close to the heliospheric nose strongly suggests that at least some of the complex structure observed in the 1992–1994 heliospheric radio emission event is due to shocks embedded within the global merged interaction region following those at the leading edge that are likely responsible for the emissions very early in the event. This possibility was suggested by *Kurth and Gurnett* [1997].

[29] The locations given by the observations associated with roll turns 6–9 are quite diverse and spread out from the

nose position. It appears as though the spectral element associated with location 6′ (the low-frequency feature) evolves into that associated with location 7. We remarked above that there are reasons to suspect locations 6 and 6′ because of the questionable applicability of the point source assumption, but location 7 was basically insensitive to this issue. Source locations 8 and 9 are on the opposite side of the nose from locations determined from roll turns 6 and 7, even though the emissions appear to be a part of the same set of transient events. On closer inspection, though, the drift rate of the spectral feature studied in roll turns 8 and 9 is significantly different from that associated with turns 6 and 7; hence this could be a separate emission element.

[30] The distribution of source locations in Figure 17 is remarkable. First, as suggested by *Gurnett et al.* [1993], the "primary" sources are generally clustered near the nose direction. This is partly a self-fulfilling result, since this was an important factor in choosing the "primary" source locations. Further, *Cairns and Zank* [2002] predict the most likely region for the source is within 20 and 50 AU of the nose. Assuming a distance of 135 AU, 50 AU translates to an angle of a little more than 20 degrees from the nose. Certainly, many of the source locations in Figure 17 are within a few tens of degrees of the nose, but several are at significantly greater distances. The most remarkable result, however, is that the spread which is apparent in the "prime" source locations extend in a line in the latitude-longitude coordinate system of Figure 17. It would be reasonable to expect some random scatter around the nose direction based on our assumptions and our model of the radio generation mechanism [*Gurnett et al.*, 1993; *Cairns and Zank*, 2002]. That these extend along a line, however, suggests an ordering which would not have been expected based on any asymmetry proposed for the interplanetary medium. That is, a linear distribution parallel to the ecliptic plane might have been suggested by the largely azimuthal orientation of the magnetic field in the outer heliosphere or by differences in the average low- and high-latitude solar wind conditions. However, the line of sources is strongly rotated from the plane of the ecliptic, hence, certainly not associated with either of these asymmetries.

[31] We are led to the hypothesis that the orientation of the external local interstellar medium (LISM) magnetic field is important in determining the preferred location for the radio sources just outside the heliopause. This would be true even in the case of a supersonic interstellar flow, since the interstellar field direction would control the direction of the magnetic field in the outer heliosheath. The interstellar magnetic field is the only known aspect of the interstellar medium which could break the symmetry of the flowing interstellar medium at its interface with the heliopause, although there could be others such as density gradients or discontinuities embedded in the ISM. We suggest that there is a preferred LISM magnetic field direction which leads to the generation of electrostatic Langmuir waves in the source, the efficient coupling of the Langmuir waves into the observed electromagnetic radio waves, or the propagation characteristics (beaming properties) of the generated waves. We note a study by *Macek* [1990] that attempted to identify the locus of points along the heliopause that presented a fixed angle between a supposed interstellar field line and the heliospheric field. This study was concerned with places where one might expect reconnection to occur. However, it was interesting that in some cases this locus presented a linear or quasi-linear locus at the heliospheric nose, not dissimilar to the one presented in Figure 17.

[32] Information on galactic magnetic fields can be derived from the rotation measures of pulsars [*Manchester and Taylor*, 1977] at distances of a few to several kpc [c.f. *Rand and Kulkarni*, 1989; *Rand and Lyne*, 1994] and from the polarization of starlight within 30 pc [c.f. *Tinbergen*, 1982]. *Heiles* [1987, 1996] reviews various methods for studying galactic magnetic fields and summarizes the results. *Frisch* [1990] also summarizes the observations of the magnetic field strength and direction in the LISM. Each of these sources suggest that there is an organized galactic magnetic field which is longitudinal in nature and parallel to the galactic plane. For example, *Rand and Lyne* [1994] infer that locally the field is directed toward a galactic longitude of 88° with a magnitude of approximately 1.4 microGauss. Of course, the sources for the underlying measurements are stars and pulsars, most of which are great distances from the Sun and even the closest are several parsecs away. Hence it is unknown whether the general longitudinal field is dominant in the LISM, although this is suggested by *Frisch* [1990]. In addition to the ordered field there are variations thought to be associated with supernova bubbles or other inhomogeneities.

[33] Figure 18 shows just the region near the nose and the collection of "primary" radio source locations. In addition, we have added the galactic plane to the plot. Remarkably, the source locations align very nearly parallel to the galactic plane, but offset so as to include the nose direction. Given that several studies noted above have concluded that the ordered component of the galactic magnetic field is parallel to the galactic plane, the unavoidable conclusion is that this is also the orientation of the field in the local interstellar medium at the interface with the heliosphere.

[34] *Gurnett and Kurth* [1996] suggest that the most likely explanation for small, isolated source regions is that the orientation of the magnetic field at the shock front is important in determining the intensity of electron beams which, in turn, generate the Langmuir waves from which the radio emissions are likely generated. In particular, they point out that at Earth's bow shock quasi-perpendicular shocks are responsible for the most intense upstream electron beams [*Anderson et al.*, 1979]. *Nelson and Robinson* [1975] use a similar argument to explain why type II radio emissions are not generated uniformly over interplanetary shocks. Let us consider the geometry of the interaction which produces the radio emissions implied by the model proposed by *Gurnett et al.* [1993]. In this model the exciter is a shock moving outward from the Sun at or just beyond the heliopause. To first order, the shock normal is likely to be more-or-less radial from the Sun and hence roughly perpendicular to the heliopause near the nose. If we assume, for the moment, that the distribution of sources in Figure 18 is evidence for a magnetic field parallel to the galactic plane, then we may also assume that the galactic field is nearly longitudinal with respect to the galactic center. The galactic longitude of the nose of the heliosphere is about 3°; hence the galactic field is perpendicular to a radially directed shock normal at the nose. In other words, the

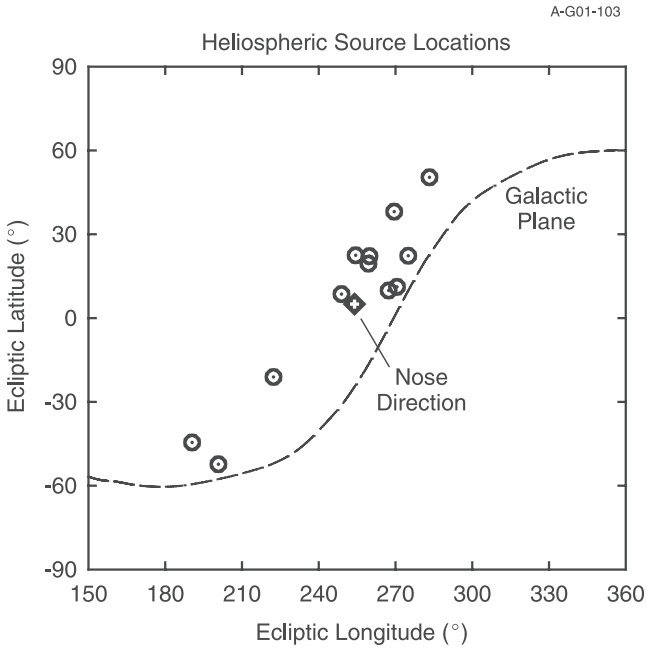

Figure 18. Here, just the prime locations are plotted along with the position of the galactic plane. It appears from this illustration that the source locations are distributed in a more-or-less linear fashion approximately parallel to the galactic plane. This would seem to suggest that an interstellar magnetic field parallel to the galactic plane through the nose of the heliosphere breaks the symmetry of the interaction. Such a field orientation is suggested by pulsar rotation measures and by observations of starlight polarization.

longitudinal configuration of the galactic field in the immediate vicinity of the heliospheric nose provides for quasi-perpendicular shocks as they enter the LISM.

[35] On the other hand, it is reasonable to assume that other interstellar field lines parallel to that intersecting the nose are in the process of convecting around the heliosphere and that there should be other field lines with similar orientation over the surface of the upstream heliopause, so it is not apparent why just the field line intersecting the nose is special.

[36] In summary, we have used a combination of three different types of source localization to determine the two-dimensional source positions for low-frequency heliospheric radio emissions in ecliptic coordinates. Most of the source locations are within a few tens of degrees of the heliospheric nose, although some sources are located as far as 90° from the nose. The distribution is roughly linear and aligned generally parallel to the galactic plane. We conclude that the magnetic field in the local interstellar medium is the only obvious means by which to impose an asymmetry to the set of source locations about the nose; it is likely these measurements confirm that the previously proposed longitudinal magnetic field configuration parallel to the galactic plane is present just upstream of the heliosphere. The apparent source sizes of the radio emissions range from very small (a few degrees at the most) to a few tens of degrees. In a couple of cases, the source half-angle could approach 80 degrees. We suggest that the true source size is quite small and that the larger sizes found here are likely due to scattering in the intervening medium. The fact that the apparent source size varies considerably implies scattering in the outer heliosphere is variable and is a function of time, position, or both.

[37] **Acknowledgments.** We are grateful to P. Frisch for providing useful references on measurements and models of the galactic magnetic field. The research at The University of Iowa was supported by the National Aeronautics and Space Administration through contract 959193 with the Jet Propulsion Laboratory.

[38] Shadia Rifai Habbal thanks William A. Coles and Priscilla C. Frisch for their assistance in evaluating this paper.

References

Ajello, J. M., A. I. Stewart, G. E. Thomas, and A. Garps, Solar cycle study of interplanetary Lyman-alpha variations: Pioneer Venus orbiter sky background results, *Ap. J.*, *317*, 964–986, 1987.

Anderson, K. A., R. P. Lin, F. Martel, C. S. Lin, G. K. Parks, and H. R'eme, Thin sheets of energetic electrons upstream from the Earth's bow shock, *Geophys. Res. Lett.*, *6*, 401–404, 1979.

Armstrong, J. W., W. A. Coles, and B. J. Rickett, Radio wave scattering in the outer heliosphere, *J. Geophys. Res.*, *105*, 5149–5156, 2000.

Baumback, M. M., Direction-finding measurements of type III radio bursts out of the ecliptic plane, M.S. thesis, The University of Iowa, Iowa City, Iowa, May 1976.

Cairns, I. H., Radio wave scattering in the outer heliosphere: Preliminary calculations, *Geophys. Res. Lett.*, *22*, 3433–3436, 1995.

Cairns, I. H., On radio wave scattering in the outer heliosphere, in *Solar Wind Eight*, *AIP Conf. Proc. 382*, edited by D. Winterhalter et al., pp. 582–585, Am. Inst. of Phys., Woodbury, N. Y., 1996.

Cairns, I. H., and G. P. Zank, Turn-on of 2–3 kHz radiation beyond the heliopause, *Geophys. Res. Lett.*, *29*(7), 1143, doi:10.1029/2001GL014112, 2002.

Frisch, P. C., Characteristics of the local interstellar medium, in *Physics of the Outer Heliosphere*, edited by S. Grzedzielski and D. E. Page, pp. 19–28, Pergamon, New York, 1990.

Gurnett, D. A., and W. S. Kurth, Heliospheric 2–3 kHz radio emissions and their relationship to large Forbush decreases, *Adv. Space Sci.*, *16*(9), 279–290, 1995.

Gurnett, D. A., and W. S. Kurth, Radio emissions from the outer heliosphere, *Space Sci. Rev.*, *78*, 53–66, 1996.

Gurnett, D. A., W. S. Kurth, S. C. Allendorf, and R. L. Poynter, Radio emission from the heliopause triggered by an interplanetary shock, *Science*, *262*, 199–203, 1993.

Gurnett, D. A., S. C. Allendorf, and W. S. Kurth, Direction-finding measurements of heliospheric 2–3 kHz radio emissions, *Geophys. Res. Lett.*, *25*, 4433–4436, 1998.

Heiles, C., Interstellar magnetic fields, in *Interstellar Processes*, edited by D. J. Hollenbach and H. A. Thronson Jr., pp. 171–194, D. Reidel, Norwell, Mass., 1987.

Heiles, C., A comprehensive view of the galactic magnetic field, especially near the Sun, in *Polarimetry of the Interstellar Medium*, *ASP Conf. Ser. 97*, edited by W. G. Roberge and D. C. B. Whittet, pp. 457–474, Astron. Soc. of the Pac. San Fransisco, Calif., 1996.

Kurth, W. S., and D. A. Gurnett, Outer heliospheric radio emissions, in *Cosmic Winds and the Heliosphere*, edited by J. R. Jokipii, C. P. Sonett, and M. S. Giampapa, pp. 793–832, Univ. of Ariz. Press, Tucson, Ariz., 1997.

Kurth, W. S., and D. A. Gurnett, Dual spacecraft measurements as a tool for determining the source of low frequency heliospheric radio emissions, in *The Outer Heliosphere: The Next Frontiers*, edited by K. Scherer et al., pp. 245–251, Pergamon, New York, 2001.

Kurth, W. S., D. A. Gurnett, F. L. Scarf, and R. L. Poynter, Detection of a radio emission at 3 kHz in the outer heliosphere, *Nature*, *312*, 27–31, 1984.

Macek, W. M., Reconnection pattern at the heliopause, in *Physics of the Outer Heliosphere*, edited by S. Grzedzielski and D. E. Page, pp. 399–402, Pergamon, New York, 1990.

Manchester, R. N., and J. H. Taylor, *Pulsars*, pp. 134–137, Freeman, San Francisco, 1977.

Nelson, G. J., and R. D. Robinson, Multi-frequency heliograph observations of type II bursts, *Proc. Astron. Soc. Aust.*, *2*, 370–373, 1975.

Rand, R. J., and S. R. Kulkarni, The local galactic magnetic field, *Ap. J.*, *343*, 760–772, 1989.

Rand, R. J., and A. G. Lyne, New rotation measures of distant pulsars in the inner galaxy and magnetic field reversals, *Mon. Not. RAS*, *268*, 497–505, 1994.

Scarf, F. L., and D. A. Gurnett, A plasma wave investigation for the Voyager mission, *Space Sci. Rev.*, *21*, 289–308, 1977.

Steinolfson, R. S., and D. A. Gurnett, Distances to the termination shock and heliopause from a simulation analysis of the 1992–93 heliospheric radio emission event, *Geophys. Res. Lett.*, *22*, 651–654, 1995.

Tinbergen, J., Interstellar polarization in the immediate solar neighbourhood, *Astron. Astrophys.*, *105*, 53–64, 1982.

W. S. Kurth and D. A. Gurnett, Department of Physics and Astronomy, University of Iowa, Iowa City, IA 52242, USA. (william-kurth@uiowa.edu; donald-gurnett@uiowa.edu)